



Dynamic stress concentration in a hybrid composite laminate subjected to a sudden internal break

E. Mirshekari* and A. Reza

Department of Mechanical Engineering, Ahvaz Branch, Islamic Azad University, Ahvaz, Iran

Article info:

Received: 26/05/2017

Accepted: 23/08/2018

Online: 26/08/2018

Keywords:

Laminate,
Crack,
Transient response,
Dynamic stress
Concentration,
Hybrid.

Abstract

In this work, transient dynamic stress concentration in a hybrid composite laminate subjected to a sudden internal crack is examined. It is assumed that all fibers lie in one direction and the applied load acts along the direction of fibers. Two types of arrangements are considered for the fiber; square and hexagonal. Using the shear lag model, equilibrium equations are deduced, and upon proper application of initial and boundary conditions, the complete field equations are obtained using finite difference method. The results of the dynamic effect of fiber breakage on stress concentration are well examined in the presence of a second fiber type. These results are compared to those of their static values in both models. The effect of surface cracks on stress concentration, as a result of fiber breakage, is also examined. The values of dynamic stress concentrations are deduced and compared to those of a lamina. Also, the peak stress concentration during transition time for fibers to reach static equilibrium is calculated and compared with those of static values.

1. Introduction

Composites have been broadly utilized in different types of applications. They can be exposed to numerous deformities such breaks, holes, or some other type of discontinuities. Disregarding the impact of such imperfections may prompt significant issues in structural entirety of the entire body. Due to heterogeneous and nonisotrop properties of composite materials, it is very hard to investigate their mechanical behavior. To understand this behavior, the material has to be modeled properly. Many studies have been done in the field of micro and Nano mechanical modeling of

composites [1-4]. One of the models available is the so-called shear lag model, wherein, all fibers are assumed to take axial load, while matrix sustains only shear. The manner of transferring of load from any broken fibers to its adjoining fibers is through shear stress created within the matrix. It is demonstrated that [5-8] Shear-Lag model gives generally exact outcomes on normal stresses created in composites with the matrix by low tensile modulus. Some authors have applied numerical methods to compare the results of shear-lag model with those of finite element analysis [9, 10]. By definition a hybrid composites is one which is composed of more than one type of filament. The stress distribution

*Corresponding author
email address: erfan.mirshekari@gmail.com

inside the material can be complicate with the existence of the second type fiber. A few researchers have likewise attempted to study the stress distribution and fracture for hybrid composites materials [11-13]. Transient response of stress distributions due to initiation of a crack in a lamina was first studied by Hedgepeth [5]. He used the conventional shear lag model to obtain equilibrium equations in a lamina with infinite dimensions and used laplace transforms to solve the equilibrium equations. Due to the complexity of the problem, he just used three broken fibers. Some other authors have used numerical approaches, namely finite difference method, to study the dynamic behavior of composites in practice [14, 15]. Reza *et al.* [16] investigated the dynamic stress concentration of a lamina using finite difference method and studied the effect of viscoelasticity of a polymer matrix on it. Souad et al. [17] investigated the stress concentration factor in a fibre reinforced composite material with ceramic matrix. Using finite element method, they calculated the stress concentration factor for crack growth in the ceramic matrix and fiber-matrix interface. Results showed that inclined crack at interface center has no more effect on stress intensity factors compared the crack at interface edge. Aboudi [18] presented a continuum model capable of generating the transient electro-elastic field in piezoelectric composites of periodic microstructure, caused by the sudden appearance of localized defects. Reza and Shishesaz [19] investigated the effect of viscoelasticity of polymeric matrix of composite materials on the transient stress concentration due to a sudden break in its fibers and used explicit finite difference method. In present work, transient distribution of stresses in a finite width hybrid composites laminate subjected to a sudden internal crack is studied. The hybridization effect, arrangement of fibers in the laminate, crack location as well size of the sudden crack on dynamic stress overshoot is well examined. The introduced transient time is defined as the time required for each fiber to

reach its static equilibrium, once the crack is initiated.

2. Derivation of formulas

To derive the necessary field equations, it is assumed that all the fibers are aligned in parallel and can take extensional load only. Each matrix bay sustains only shear stress. This is a good assumption in most composites with a phenolic resin or weak in tension. Furthermore, it is assumed that the laminate is subjected to a tensile load with the magnitude of P, applied at infinity.

To derive equilibrium equations, additional assumptions are made as follow:

- There is a perfect bound between each fiber and its neighboring matrix bays.
- All fibers behave as linear elastic up to the point of fracture.
- Fibers and matrix are assumed to be homogeneous.

In the derivation of formulas, two types of fiber arrangement are postulated in the laminate. These arrangements are discussed separately in the subsequent sections.

2.1 Hybrid Square Arrangement

Fig. 1 shows the cross section of a laminate with a square arrangement. Here, "d" represents the spacing between any two adjacent fibers while *x* is measured along the direction of filaments. Coordinate axes *y* and *z* are taken to be normal to fibers as shown.

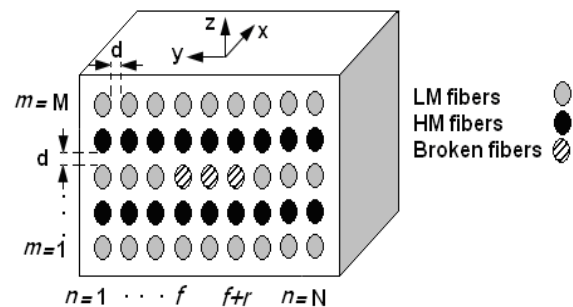


Fig. 1. Cross section of a hybrid laminate with a square arrangement for fibers.

According to Fig. 1, n represents the number of any fiber in any layer, ranging from 1 to N . Moreover, m corresponds to the number of layers, ranging from 1 to M . For this type of fiber arrangement, each filament is influenced by four shear stresses from the neighboring fibers. The laminate edge can end in an LM (low modulus) or an HM (high modulus) fiber. It is assumed that the type of fibers in every other row is the same. The asterisk symbol (*) is used to highlight the properties associated with LM fibers.

The crack can initiate at $x=0$, within the f_m^{th} layer, from the f^{th} fiber, while r corresponds to the total number of broken fibers. Using linear elasticity equations, one can show that the force balance in any LM fiber (see Fig. 2) results into;

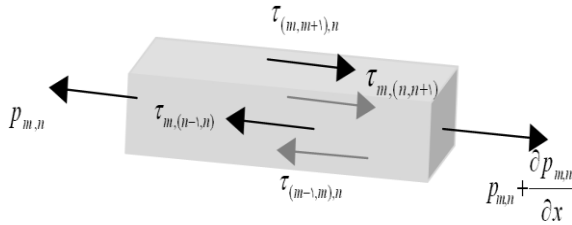


Fig. 2. Force equilibrium on a portion of low modulus fiber in a square arrangement.

$$\frac{\partial p_{m,n}^*}{\partial x} dx + \left\{ \begin{array}{l} \tau_{m,(n,n+1)} - \tau_{m,(n-1),n} + \tau_{m,(m+1),n} \\ - \tau_{m,(m-1),n} \end{array} \right\} h \cdot dx = (m^* \cdot dx) a_{m,n}^* \quad (1)$$

In the above equation, m^* is mass per unit length of an LM fiber while $a_{m,n}^*$ is its corresponding acceleration value. Substituting shear stresses in terms of fiber displacement, differential-difference Eq. (1), may be written as:

$$E_f^* A_f^* \frac{\partial^2 u_{m,n}^*}{\partial^2 x} + \frac{Gh}{d} (u_{m,n+1}^* + u_{m,n-1}^* + u_{m+1,n}^* + u_{m-1,n}^* - 4u_{m,n}^*) = m^* \frac{\partial^2 u_{m,n}^*}{\partial^2 t} \quad (2)$$

A similar expression may be written for an HM as;

$$E_f A_f \frac{\partial^2 u_{m,n}}{\partial^2 x} + \frac{Gh}{h} (u_{m,n+1} + u_{m,n-1} + u_{m+1,n}^* + u_{m-1,n}^* - 4u_{m,n}) = m \frac{\partial^2 u_{m,n}}{\partial^2 t} \quad (3)$$

The equilibrium equations for the edge fibers may be written using the same procedure. In a matrix notation, the equilibrium equations for the whole laminate may be written as;

$$e u'' - \frac{Gh}{d} L_1 u = m \ddot{u} \quad (4)$$

Displacement vector u has the order of $M \times N$ and is defined as in Eq. (5). Moreover, u'' and \ddot{u} correspond to the derivative of u with respect to x and time respectively.

$$u^T = [u_{1,1}^*, u_{1,2}^*, \dots, u_{1,N}^*, u_{2,1}, u_{2,2}, \dots, u_{2,N}, \dots, u_{M,1}^*, \dots, u_{M,N}^*] \quad (5)$$

The coefficient matrices m , e and L_1 are expressed as;

$$e = \begin{bmatrix} \begin{bmatrix} E_f A_f & 0 & 0 \\ \dots & \vdots & \dots \\ 0 & 0 & E_f A_f \end{bmatrix} & 0 & \dots & 0 \\ 0 & \begin{bmatrix} E_f^* A_f^* & 0 & 0 \\ \dots & \vdots & \dots \\ 0 & 0 & E_f^* A_f^* \end{bmatrix} & \dots & 0 \\ \vdots & \vdots & \dots & 0 \\ 0 & 0 & 0 & \begin{bmatrix} E_f A_f & 0 & 0 \\ \dots & \vdots & \dots \\ 0 & 0 & E_f A_f \end{bmatrix} \end{bmatrix}_{(K \times K)} \quad (6)$$

$$L_I = \begin{bmatrix} [A_1] & [I] & 0 & \dots & 0 & 0 & 0 \\ [I] & [B_1] & [I] & \dots & 0 & 0 & 0 \\ 0 & [I] & [B_1] & \dots & 0 & 0 & 0 \\ \vdots & \vdots & \vdots & \dots & \vdots & \vdots & \vdots \\ 0 & 0 & 0 & \dots & [B_1] & [I] & 0 \\ 0 & 0 & 0 & \dots & [I] & [B_1] & [I] \\ 0 & 0 & 0 & \dots & 0 & [I] & [A_1] \end{bmatrix}_{(K \times K)} \quad (7)$$

In Eq. (7), K is equal to M×N and **I** is the Nth order identity matrix. Moreover, matrices **A_I** and **B_I** are equal to;

$$A_I = \begin{bmatrix} -2 & 1 & 0 & \dots & 0 & 0 & 0 \\ 1 & -3 & 1 & \dots & 0 & 0 & 0 \\ 0 & 1 & -3 & \dots & 0 & 0 & 0 \\ \vdots & \vdots & \vdots & \dots & \vdots & \vdots & \vdots \\ 0 & 0 & 0 & \dots & -3 & 1 & 0 \\ 0 & 0 & 0 & \dots & 1 & -3 & 1 \\ 0 & 0 & 0 & \dots & 0 & 1 & -2 \end{bmatrix}_{(N \times N)}, \quad (8)$$

$$B_I = \begin{bmatrix} -3 & 1 & 0 & \dots & 0 & 0 & 0 \\ 1 & -4 & 1 & \dots & 0 & 0 & 0 \\ 0 & 1 & -4 & \dots & 0 & 0 & 0 \\ \vdots & \vdots & \vdots & \dots & \vdots & \vdots & \vdots \\ 0 & 0 & 0 & \dots & -4 & 1 & 0 \\ 0 & 0 & 0 & \dots & 1 & -4 & 1 \\ 0 & 0 & 0 & \dots & 0 & 1 & -3 \end{bmatrix}_{(N \times N)}$$

2.2 Hybrid hexagonal arrangement

Fig. 3 depicts a hexagonal arrangement of fibers in the hybrid composite laminate. Each fiber is surrounded by six filaments. The coordinates *m* and *n* are as shown in the figure. Using the shear lag model along with linear elasticity equations, the equilibrium equation in the *n*th LM fiber in the *m*th layer results into;

$$\begin{aligned} & \{ \tau_{m,(n,n+1)} - \tau_{m,(n-1,n)} + \tau_{(m,m+1),n} - \tau_{(m-1,m),n} \\ & \quad + \tau_{(m+1,m),(n,n-1)} \\ & - \tau_{(m-1,m),(n,n+1)} \} h \cdot dx + \frac{\partial p_{m,n}}{\partial x} dx \quad (9) \\ & = (m \, dx) a_{m,n} \end{aligned}$$

The above equation may be written in terms of fiber displacements as;

$$E_f A_f^* \frac{\partial^2 u_{m,n}^*}{\partial^2 x} + \frac{Gh}{d} (u_{m,n+1}^* + u_{m,n-1}^* + u_{m+1,n}^* + u_{m-1,n}^* + u_{m-1,n+1}^* + u_{m+1,n-1}^* - 6u_{m,n}^*) - m^* \frac{\partial^2 u_{m,n}^*}{\partial^2 t} \quad (10)$$

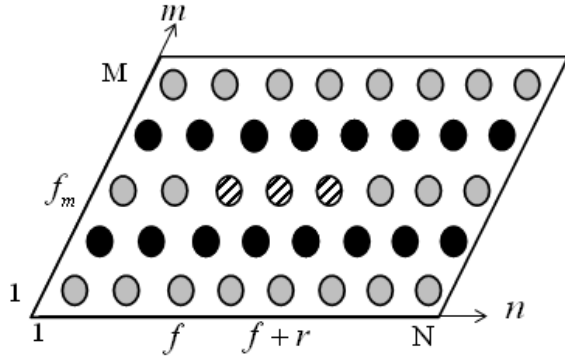


Fig. 3. Cross section of a hybrid laminate with hexagonal arrangement for fibers.

A similar equation may be written for HM fibers. Similar to that of square arrangement, equilibrium equations for the edge fibers may be written as well. In a matrix notation, the equilibrium equations for the whole laminate may be represented as;

$$eu'' - \frac{Gh}{d} L_2 u'' = m\ddot{u} \quad (11)$$

where matrix L_2 is equal to;

$$L_2 = \begin{bmatrix} [A_2] & [J]^T & [0] & \dots & [0] & [0] & [0] \\ [J] & [B_2] & [J]^T & \dots & [0] & [0] & [0] \\ [0] & [J] & [B_2] & \dots & [0] & [0] & [0] \\ \vdots & \vdots & \vdots & \dots & \vdots & \vdots & \vdots \\ [0] & [0] & [0] & \dots & [B_2] & [J]^T & [0] \\ [0] & [0] & [0] & \dots & [J] & [B_2] & [J]^T \\ [0] & [0] & [0] & \dots & [0] & [J] & [C] \end{bmatrix}_{(K \times K)} \quad (12)$$

Parameter K is defined as mentioned above. Matrices A_2, B_2, C and J are equal to:

$$\begin{aligned} A_2 &= \begin{bmatrix} -2 & 1 & 0 & \dots & 0 & 0 & 0 \\ 1 & -4 & 1 & \dots & 0 & 0 & 0 \\ 0 & 1 & -4 & \dots & 0 & 0 & 0 \\ \vdots & \vdots & \vdots & \dots & \vdots & \vdots & \vdots \\ 0 & 0 & 0 & \dots & -4 & 1 & 0 \\ 0 & 0 & 0 & \dots & 1 & -4 & 1 \\ 0 & 0 & 0 & \dots & 0 & 1 & -3 \end{bmatrix}_{(N \times N)} \\ B_2 &= \begin{bmatrix} -4 & 1 & 0 & \dots & 0 & 0 & 0 \\ 1 & -6 & 1 & \dots & 0 & 0 & 0 \\ 0 & 1 & -6 & \dots & 0 & 0 & 0 \\ \vdots & \vdots & \vdots & \dots & \vdots & \vdots & \vdots \\ 0 & 0 & 0 & \dots & -6 & 1 & 0 \\ 0 & 0 & 0 & \dots & 1 & -6 & 1 \\ 0 & 0 & 0 & \dots & 0 & 1 & -4 \end{bmatrix}_{(N \times N)} \\ C &= \begin{bmatrix} -3 & 1 & 0 & \dots & 0 & 0 & 0 \\ 1 & -4 & 1 & \dots & 0 & 0 & 0 \\ 0 & 1 & -4 & \dots & 0 & 0 & 0 \\ \vdots & \vdots & \vdots & \dots & \vdots & \vdots & \vdots \\ 0 & 0 & 0 & \dots & -4 & 1 & 0 \\ 0 & 0 & 0 & \dots & 1 & -4 & 1 \\ 0 & 0 & 0 & \dots & 0 & 1 & -2 \end{bmatrix}_{(N \times N)} \\ J &= \begin{bmatrix} 1 & 1 & 0 & \dots & 0 & 0 & 0 \\ 0 & 1 & 1 & \dots & 0 & 0 & 0 \\ 0 & 0 & 1 & \dots & 0 & 0 & 0 \\ \vdots & \vdots & \vdots & \dots & \vdots & \vdots & \vdots \\ 0 & 0 & 0 & \dots & 1 & 1 & 0 \\ 0 & 0 & 0 & \dots & 0 & 1 & 1 \\ 0 & 0 & 0 & \dots & 0 & 0 & 1 \end{bmatrix}_{(N \times N)} \end{aligned} \quad (13)$$

3. Initial and boundary conditions

Before any crack initiation, the normal load in any fiber equals its applied value at $x = \infty$. This means that,

$$p_{m,n}(x, 0) = p \quad (14)$$

Moreover, at the moment of fiber and matrix breakage, the instantaneous velocity of the cut fibers equals zero. This corresponds to;

$$\frac{\partial u_{m,n}}{\partial t}(x, 0) = 0 \quad (15)$$

Due to symmetry (crack initiates at $x = 0$), the displacement in all intact fibers at any time may be written as;

$$u_{m,n}(0,t) = 0 \begin{cases} (n < f \text{ or } n > r + f) \\ \text{and } (m = f_m) \\ (1 \leq n \leq N) \quad \& \quad (m \neq f_m) \end{cases} \quad (16)$$

Moreover, the load in the broken fibers after the cut is;

$$p_{m,n}(0,t) = 0 \quad (m = f_m \ \& \ f \leq n \leq r + f) \quad (17)$$

Also, as x approaches infinity, the normal load in any fiber must approach its applied value. This means that in the presence of a crack;

$$(p_{m,n})_{x \rightarrow \infty} = p \quad (18)$$

4. Non- dimensional parameters

Differential Eqs. (4 and 11) may be written in a non-dimensional form, using the following non-dimensional parameters:

$$\begin{aligned} P_n &= \frac{p_n}{p}, & P_n^* &= \frac{p_n^*}{p}, \\ Q &= \frac{m^*}{m}, & R &= \frac{E_f^* A_f^*}{E_f A_f}, \\ \frac{1}{\eta} &= \frac{d}{h} = \frac{V_m}{V_f} \\ U_n &= \sqrt{\frac{E_f A_f Gh}{p^2 d}} u_n, \\ U_n^* &= \sqrt{\frac{E_f A_f Gh}{p^2 d}} u_n^*, \\ \xi &= \sqrt{\frac{Gh}{E_f A_f d}} x, & \tau &= \sqrt{\frac{Gh}{md}} t \end{aligned} \quad (19)$$

By definition, V_f and V_m are fiber and matrix volume fractions in the lamina, respectively. In Eq. (19), Gh is the effective matrix shear stiffness and t is the transient time. Upon the application of these parameters, equilibrium Eqs. (4 and 11) may be written in a non-dimensional form as;

$$EU'' - \eta L_1 U = M\ddot{U} \quad (\text{Square arrangement}) \quad (20)$$

$$EU'' - \eta L_2 U = M\ddot{U} \quad (\text{Hexagonal arrangement}) \quad (21)$$

Matrices M and E correspond to the non-dimensional form of Eqs. (6 and 7), respectively. Furthermore, the initial boundary and boundness conditions in a non-dimensional form reduce into;

$$\frac{\partial U_{m,n}}{\partial \tau}(\xi, 0) = 0 \quad (22)$$

$$P_{m,n}(\xi, 0) = \frac{\partial U_{m,n}}{\partial \xi}(\xi, 0) = 1 \quad (23)$$

$$U_{m,n}(0, \tau) = 0 \begin{cases} (n < f \text{ or } n > r + f) \\ \& \ (f_m \leq m \leq l + f_m) \\ (1 \leq n \leq N) \\ \& \ (m < f_m \text{ or } m > l + f_m) \end{cases} \quad (24)$$

$$P_{m,n}(0, \tau) = \frac{\partial U_{m,n}}{\partial \xi}(0, \tau) = 0 \quad (25)$$

$$\begin{aligned} (f \leq n \leq r + f) \\ \& \ f_m \leq m \leq l + f_m \end{aligned}$$

$$(P_{m,n})_{\xi \rightarrow \infty} = 1 \quad (26)$$

5. Finite difference solution of equilibrium equations

Equilibrium Eqs. (20 and 21) are much alike except for the coefficient matrices L_1 and L_2 . Hence, the solution method presented covers both cases. Moreover, these equations form a set of equations with two variables. Now,

introducing $v=N(m-1)+n$, one may write the elements of the U matrix as;

$$U_{m,n} = \bar{U}_v \quad (27)$$

To solve equilibrium equations, it is assumed that each fiber has a finite length L which can be divided into equal segments with the size of $\Delta\xi$ (See Fig. 4) such that,

$$L = S_z \Delta\xi \quad (28)$$

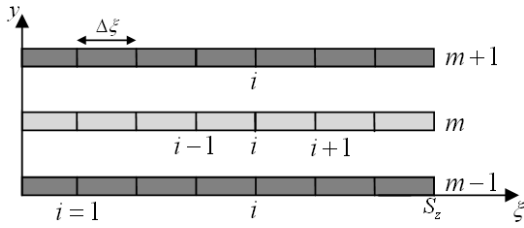


Fig. 4. Finite difference grid of composite fibers.

In Eq. (29), S_z corresponds to the number of divisions selected on each fiber. Labeling each segment by i , one may write,

$$\xi_i = i\Delta\xi \quad (29)$$

Labeling each time step $\square\square$ by j , we may write;

$$\tau_j = j\Delta\tau \quad (30)$$

Denoting S_t as the number of time segments between the state of crack initiation and that of static equilibrium, then, the total transient time is given by;

$$\tau_{total} = S_t \Delta\tau \quad (31)$$

Using central difference about point i , each term in equilibrium Eq. (20) is written in a finite difference form as follow;

$$\frac{\partial^2 \bar{U}_v^{i,j}}{\partial \xi^2} = \frac{\bar{U}_v^{i+1,j} - 2\bar{U}_v^{i,j} + \bar{U}_v^{i-1,j}}{(\Delta\xi)^2} \quad (32)$$

Here, a term such as $\bar{U}_v^{i,j}$ corresponds to the displacement of n^{th} fiber in the m^{th} layer, (at a distance $\xi = i\Delta\xi$ from the center of n^{th} fiber) at time $\tau = j\Delta\tau$, after the crack initiation.

Similarly, the partial derivative of $U_n^{i,j}$ with respect to the time may be written as;

$$\frac{\partial^2 \bar{U}_v^{i,j}}{\partial \tau^2} = \frac{\bar{U}_v^{i,j+1} - 2\bar{U}_v^{i,j} + \bar{U}_v^{i,j-1}}{(\Delta\tau)^2} \quad (33)$$

Using Eqs. (32 and 33), the differential-difference Eq. (21) may be written in a finite difference form as;

$$\begin{aligned} \bar{U}_v^{i,j+1} = & \frac{(\Delta\tau)^2}{M_{v,v}} \sum_{k=1}^{M \times N} \eta \bar{L}_{v,k} \bar{U}_k^{i,j} \\ & - 2 \left(1 - \frac{s \bar{E}_{v,v}}{M_{v,v}} \right) \bar{U}_v^{i,j} + \frac{s \bar{E}_{v,v}}{M_{v,v}} \bar{U}_v^{i,j+1} \\ & + \frac{s \bar{E}_{v,v}}{M_{v,v}} \bar{U}_v^{i-1,j} - \bar{U}_v^{i,j-1} \end{aligned} \quad (34)$$

where;

$$s = \left(\frac{\Delta\tau}{\Delta\xi} \right)^2 \quad (35)$$

Eq. (34) expresses the displacement of i^{th} portion of $(m,n)^{th}$ fiber at the $(j+1)^{th}$ time step. Due to the presence of the terms $\bar{U}_v^{i,j}$ and $\bar{U}_v^{i,j-1}$, it is necessary to calculate the displacement of the corresponding portions of the fiber at the first two time steps ($j=1$ and $j=2$), using initial conditions [20].

Application of first forward difference to Eq. (23) leads into;

$$P_v(\xi, 0) = \frac{\partial \bar{U}_v}{\partial \xi}(\xi, 0) = \frac{\bar{U}_v^{(i+1,1)} - \bar{U}_v^{(i,1)}}{\Delta\xi} = 1 \quad (36)$$

Taking advantage of symmetry in the laminate, the mid-center displacement of all fibers at the first time step ($i=1$) equals zero. This means that

$\bar{U}_v^{(1,1)} = 0$. Using this concept along with Eq. (36), displacements in all portions of fibers at the first time step ($j=1$) are equal to;

$$\begin{aligned} \bar{U}_v^{(2,1)} &= \Delta\xi, \quad \bar{U}_v^{(3,1)} = 2\Delta\xi, \dots, \\ \bar{U}_v^{(S_z,1)} &= (S_z - 1)\Delta\xi \end{aligned} \quad (37)$$

$1 \leq v \leq M \times N$

At the next time step, where crack initiation starts, displacements in other portions of each fiber may be obtained using Eq. (22). Using the first forward difference, we have;

$$\frac{\partial \bar{U}_v}{\partial \tau}(\xi, \Delta\tau) = \frac{\bar{U}_v^{(i,2)} - \bar{U}_v^{(i,1)}}{\Delta\tau} = 0 \quad (38)$$

Hence, the displacement at the second time step ($j=2$) may be written as;

$$\bar{U}_v^{(i,2)} = \bar{U}_v^{(i,1)} \quad 1 \leq v \leq M \times N, \quad 1 \leq i \leq S_z \quad (39)$$

Using boundary condition (24), displacement in all intact fibers, at $\square\square\square$, may be written as;

$$\bar{U}_v^{0,j} = 0 \quad (3 \leq j) \quad \& \begin{cases} (n < f \text{ or } n > r + f) \\ \& (f_m \leq m \leq l + f_m) \\ (1 \leq n \leq N) \\ \& (m < f_m \text{ or } m > l + f_m) \end{cases} \quad (40)$$

Displacement of any broken fiber at any time τ , may be obtained using boundary condition (27). To write the first order derivative of $U_{m,n}$ with respect to ξ at point $i=1$, the central difference is used instead. This results in a truncation error with the order of $(\Delta\xi)^2$ as opposed to that of $(\Delta\xi)$ for the former. Hence, displacement in the second time step ($j=2$) is obtained as follows;

$$P_v(0, \tau) = \frac{\partial \bar{U}_v}{\partial \xi}(0, \tau) = \frac{\bar{U}_v^{(2,j)} - \bar{U}_v^{(0,j)}}{2\Delta\xi} = 0 \quad (41)$$

$(3 \leq j) \text{ and } (f \leq n \leq f+r \text{ and } m = f_m)$

Upon proper substitution of the results from Eqs. (40 and 41) into Eq. (34), displacement in the intact and broken fibers at $\xi_1 = \Delta\xi$ may be written as;

$$\begin{aligned} \bar{U}_v^{1,j+1} &= \frac{(\Delta\tau)^2}{M_{v,v}} \sum_{k=1}^{M \times N} \eta \bar{L}_{v,k} \bar{U}_k^{1,j} \\ &\quad - 2 \left(1 - \frac{s\bar{E}_{v,v}}{M_{v,v}} \right) \bar{U}_v^{1,j} \\ &\quad + \frac{s\bar{E}_{v,v}}{M_{v,v}} U_v^{2,j} - U_v^{1,j-1} \end{aligned} \quad (42)$$

$$\begin{cases} (n < f \quad n > r + f) & (f_m \leq m \leq l + f_m) \\ (1 \leq n \leq N) & (m < f_m \quad m > l + f_m) \end{cases}$$

$$\begin{aligned} \bar{U}_v^{1,j+1} &= \frac{(\Delta\tau)^2}{M_{v,v}} \sum_{k=1}^{M \times N} \eta \bar{L}_{v,k} \bar{U}_k^{1,j} \\ &\quad - 2 \left(1 - \frac{s\bar{E}_{v,v}}{2M_{v,v}} \right) \bar{U}_v^{1,j} \\ &\quad + \frac{s\bar{E}_{v,v}}{M_{v,v}} U_v^{2,j} - U_v^{1,j-1} \end{aligned} \quad (43)$$

$(f \leq n \leq f+r \quad f_m \leq m \leq l + f_m)$

Once displacements at the first two time steps ($j=1, 2$) are determined from Eqs. (38 and 39), from the third time step on, their magnitudes at any other point (except for the points in y-z plane of symmetry perpendicular to the direction of fibers, see Fig. 1), can be obtained using Eq. (37). The corresponding displacements in the mid-layer are obtained from Eqs. (42 and 43). By definition, stress concentration factor K_r is the ratio of the local load to that applied at infinity. Using this definition, along with the non-dimensional form of the applied load described in Eq. (24), one may solve for the instantaneous stress concentration in the laminate using the following equation:

$$K_r = \frac{\partial U_{m,(f+r+1)}}{\partial \xi}(0, \tau) = \frac{U_{m,(f+r+1)}^{(2,j)} - U_{m,(f+r+1)}^{(1,j)}}{\Delta\xi} \quad (44)$$

The maximum value of K_r for any crack size is called dynamic stress concentration K_d . The ratio of K_d to that of its static value (K_s) is called dynamic overshoot η_r . A similar procedure may be adapted to solve Eq. (21).

6. Results and discussion

Using MATLAB programming language, displacement fields in each fiber, at the onset of fiber breaks is obtained at each time step. This process is continued until static equilibrium is reached within each filament. The mechanical properties of each lamina used in the analysis are given in Table 1.

Table 1. Mechanical properties of selected materials in the hybrid laminate.

Material	E_f (GPa)	Density, ρ (kg/m ³)
Graphite fiber (HM)	250	13.8
Glass fiber type S (LM)	86	24.4

6.1 Single type fiber laminate

To deduce the results on a non-hybrid composite (a laminate with a single type fiber), the ratio of LM to HM stiffness, namely R , as well as Q (the ratio of mass per unit length), is set equal to 1. To check the accuracy of the results based on the present work, M or the total number of layers is set equal to 1. The deduced results for a non-hybrid composite lamina are then compared to those presented by Hedgepeth in Ref. [5]. Fig. 5 shows the effect of crack size (number of broken fibers) on dynamic stress concentration in the lamina at the transient time. The total number of fibers in the lamina is assumed to be 25. Here, crack emanates from center fiber and is normal to the filaments. The results in Ref. [5] are only presented for r (total number of broken fibers) up to 3. A close match is observed between the two cases.

To further expand the results to a laminate with 21 layers, it is assumed each layer is composed of 25 filaments. Furthermore, a square

arrangement is postulated for the fibers while it is assumed the crack emanates in the mid-layer and moves symmetrically toward the edges.

According to Fig. 6, for a sudden crack with $r=5$, maximum dynamic stress concentration occurs in the intact fiber embedded in the first intact layer (on the top or bottom of the cracked layer), within a fiber next to the center of the crack. This value reads to be $K_d=1.53$. Compared to static stress concentration ($K_s=1.30$) this shows 18% increase. Simultaneously, the dynamic stress concentration at the first intact fiber bounding the crack tip happens to be $K_d=1.30$. Compared to static stress concentration ($K_s=1.21$), this shows 7.5% increase.

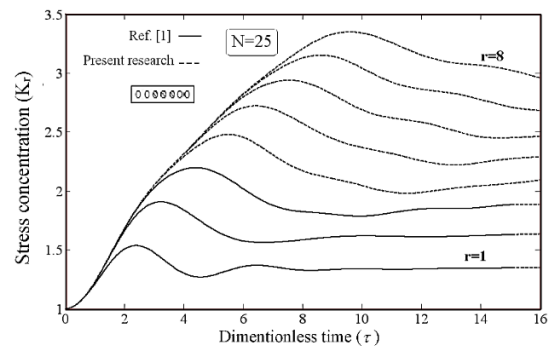


Fig. 5. The effect of crack size on dynamic stress concentration in the first intact fiber bonding the crack tip in lamina.

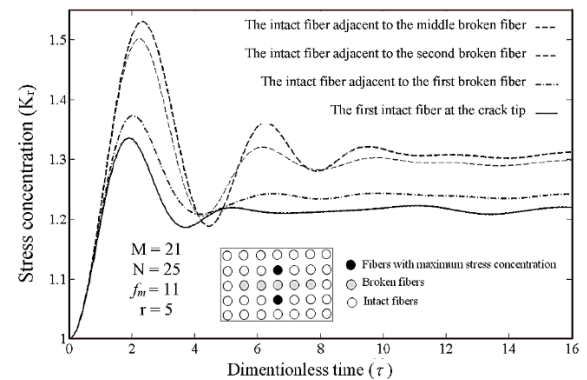


Fig. 6. Dynamic stress concentration in the intact layers bonding the crack for a square arrangement of fibers.

The effect of crack location on dynamic overshoot is shown in Fig. 7. It is observed that cracks in the first layer (top or bottom) can

increase the dynamic stress concentration by almost 7%. Cracks further away from these two layers have no effect on K_d .

Fig. 8 represents the effect of crack size on maximum dynamic stress concentration in the laminate. According to this figure, as r increases, the dynamic overshoot reaches a steady value of 1.17. Fig. 9 shows similar behavior for a hexagonal arrangement of fibers as crack size increases. Except that for small cracks, the dynamic overshoot seems to be smaller. As the number of broken fibers (crack size) increases, the dynamic overshoot reaches a steady value of 1.17.

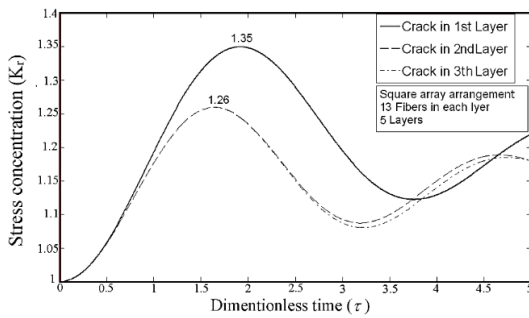


Fig. 7. The effect of crack location on dynamic stress concentration.

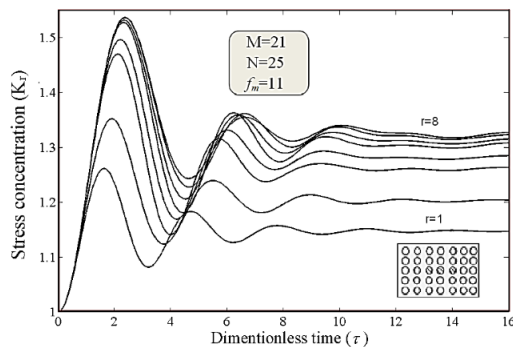


Fig. 8. The effect of crack size on dynamic stress concentration in the intact fiber adjacent to the middle broken fiber (square arrangement of fibers).

Table 2 compares the results obtained on dynamic and static stress concentration within a lamina, and that of a laminate with both hexagonal and square arrangements. Here it is assumed that $M=20$ and $N=25$. It is realized that for the same crack size, the peak dynamic stress in a lamina is more than that predicted within a laminate. For example, for $r=3$, the value of

dynamic stress concentration within a lamina is almost 1.5 times larger than that of a laminate. Examining the results on this table reveals that except for $r=1$, the magnitudes of dynamic stress concentrations for moderate crack sizes are higher in a hexagonal arrangement, as compared to those of square arrangement. For large crack sizes, the results seem to be the same.

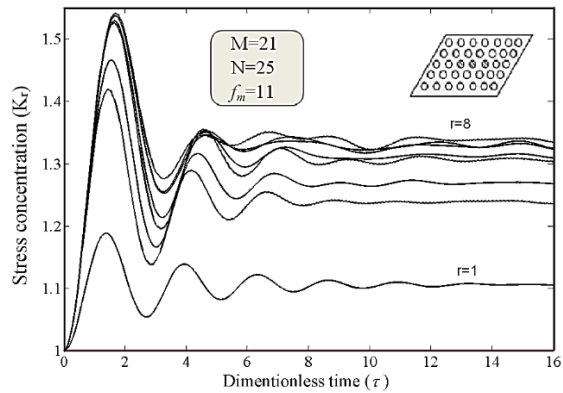


Fig. 9. The effect of crack size on dynamic stress concentration in the intact fiber adjacent to the middle broken fiber (hexagonal arrangement of fibers).

Table 2. Comparisons of the dynamic and static stress concentration factor in a lamina and a single type composite laminate.

r	Lamina		Square array laminate		Hexagonal array laminate	
	K_d	K_s	K_d	K_s [6]	K_d	K_s [6]
1	1.53	1.33	1.26	1.15	1.19	1.10
2	1.91	1.60	1.35	1.20	1.42	1.22
3	2.2	1.83	1.47	1.26	1.47	1.23
4	2.5	2.03	1.50	1.28	1.47	1.28
5	2.70	2.22	1.53	1.30	1.53	1.31
6	2.94	2.39	1.53	1.31	1.53	1.33
7	3.15	2.55	1.54	1.32	1.54	1.33
8	3.35	2.70	1.54	1.32	1.54	1.33

6.2 Hybrid laminate

To obtain the effect of a sudden crack on dynamic stress concentration in a hybrid composite laminate, the following properties in

Table 1 are used for the fibers. For the hybrid laminate, "R", or the ratio of LM to HM fiber extensional stiffnesses is set equal to 0.33. This assumption holds true for a hybrid composite with intermingled glass (as LM) and graphite (as HM) fibers.

6.2.1 Square arrangement of fibers

To deduce the results presented on Figs. 10 and 11, it has been assumed that $M=20$ and $N=25$. The crack cuts through one layer and emanates from an HM fiber at the center while bonded by an HM fiber at its tips. For a square arrangement, this means that an LM fiber experiences the peak stress concentration which takes place in the middle of the layer above the crack. According to Fig. 10, for breaks more than 3 fibers, there appears to be no change in peak dynamic stress concentration.

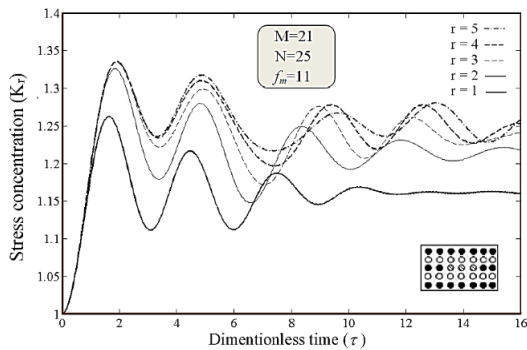


Fig. 10. The effect of crack size on dynamic stress concentration at the crack tip due to a sudden crack in hybrid laminate with square arrangement.

According to Fig. 11, for the same crack size, the peak dynamic stress concentration in the top layer adjacent to the crack is much higher than that at the crack tip. This behavior was also observed in a laminate with single type fiber. The peak dynamic overshoot in LM fibers, as compared to that of a single type fiber, increases as the laminate is hybridized. For example, according to Table 1, for $r=5$, the peak dynamic stress concentration in the first top layer (adjacent to the crack) is 1.52, while Fig. 11 shows a value of 2.14. This corresponds to a 29% increase in K_d .

Now lets consider a case in which a crack emanates in an LM layer. In this case, the top and

bottom layers are composed of HM fibers. The results for this case are shown in Figs. 12 and 13. The results in Fig. 12, correspond to peak dynamic overshoot value of 1.33 at the crack tip, while according to Fig. 13, a value of 1.22 is obtained at the top or bottom layer. This shows an increase of 8.3% in a dynamic stress concentration. Hence, hybridization effect tends to even out peak dynamic overshoot within the laminate. According to Fig. 14, an increase in volume fraction ratio (V_m/V_f) only advances the occurrence of peak K_r without changing its magnitude. Also, for cracks emanating at the first top layer, the peak value of K_r shows a higher value compared to that of an inner crack. For example, according to Fig. 15, for a square arrangement, for a surface crack with $r = 1$ (crack at the first top layer), the peak value of K_r is 1.35 while for the inner cracks (cracks at the second or any other inner layer) constant peak value of 1.26 is obtained.

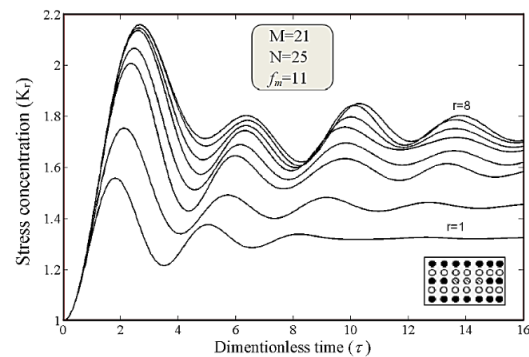


Fig. 11. The effect of crack size on peak dynamic stress concentration on the crack top layer due to a sudden crack in the hybrid laminate with square arrangement.

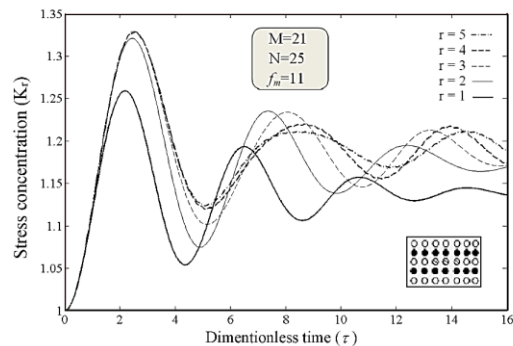


Fig. 12. The effect of crack size on dynamic overshoot in the first intact LM fiber at the crack tip for a hybrid composite laminate.

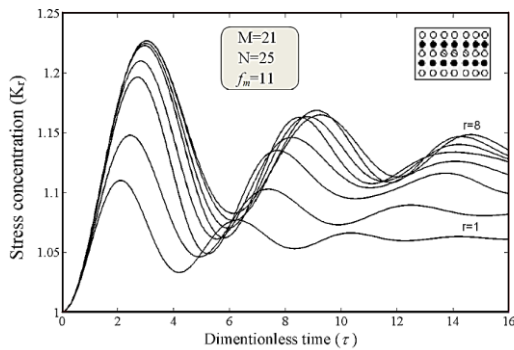


Fig. 13. The effect of crack size on dynamic overshoot in the intact HM fibers in the top layer adjacent to the crack in the hybrid composite laminate.

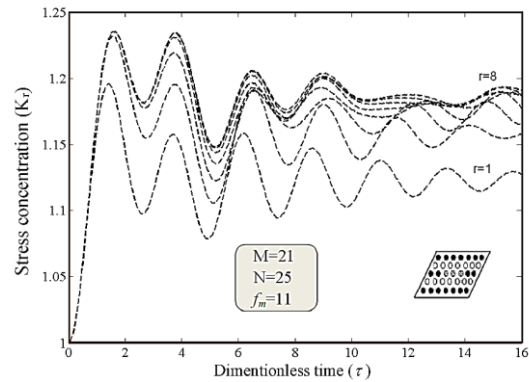


Fig. 15. The effect of crack size on dynamic stress concentration in HM fibers at the crack tip due to a sudden crack in hybrid laminate with hexagonal arrangement.

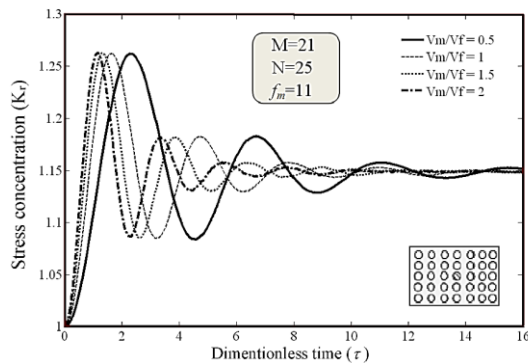


Fig. 14. The effect of volume fractions ratio on dynamic stress distribution.

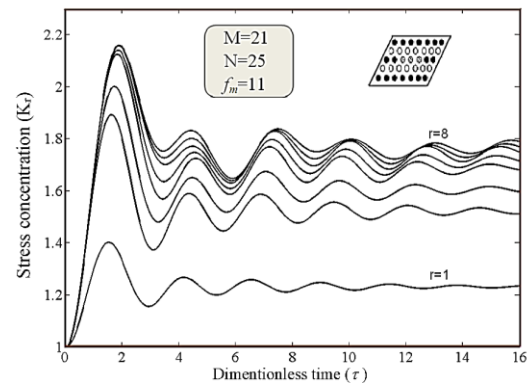


Fig. 16. The effect of crack size on dynamic stress concentration in the top layer adjacent to the crack due to a sudden break in the HM layer with hexagonal arrangement of fibers.

6.2.2 Hexagonal arrangement of fibers

According to Figs. 15-18, similar behavior is observed for the hexagonal arrangement of fibers. Figs. 15 and 16 show the dynamic stress concentration at the crack tip and the top layer adjacent to the crack, respectively. Here, the crack initiates from an HM layer. Comparison of the results in Figs. 15 and 10 reveals that the dynamic stress concentration at the crack tip is less for the hexagonal arrangement of fibers. This reduction is almost 7.5% at $r=5$. Also, a close comparison of Figs. 16 and 11 reveals that this behavior occurs for smaller cracks.

Figs. 17 and 18 show similar behavior where the cracked layer is composed of LM fibers. Fig. 17 shows the dynamic stress concentration at the crack tip while in Fig. 18, the deduced values correspond to those at the top layer adjacent to the cracked layer.

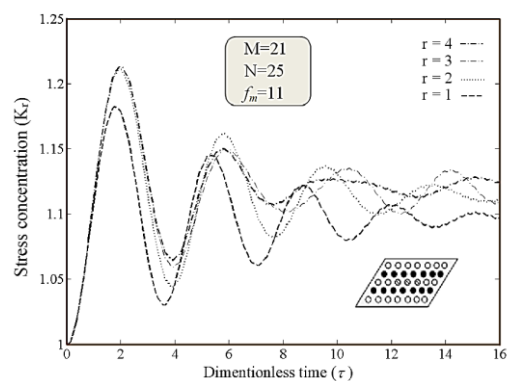


Fig. 17. The effect of crack size on dynamic stress concentration in LM fibers at the crack tip due to a sudden break in hybrid laminate with hexagonal arrangement.

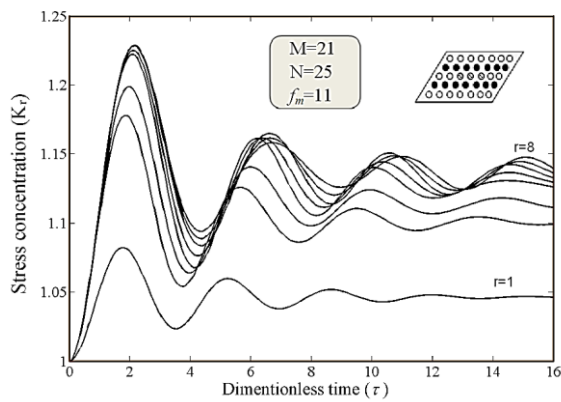


Fig. 18. The effect of crack size on dynamic stress concentration in the top layer adjacent to the crack due to a sudden crack in the LM layer with hexagonal arrangement for fibers.

7. Conclusions

The effect of a sudden crack initiation both in a single type and hybrid unidirectional laminate is studied in this research. The values of dynamic stress concentrations are deduced and compared to those of a lamina. Also, the peak stress concentration during transition time for fibers to reach static equilibrium is calculated and compared with those of static values. The effect of fiber arrangement on dynamic overshoot as well as edge effect is also examined. According to the results, for similar crack sizes, the values of static stress concentrations in a lamina are much below those obtained in a laminate. For example, for three broken fibers, the dynamic stress concentration has a value of $K_d = 2.2$ in the lamina, while for a laminate a value of $K_d = 1.47$ is obtained. Moreover, for small cracks, a laminate (with 20 layers and 25 fibers in each layer), with square arrangement of fibers results into higher values of dynamic stress concentration. For larger crack sizes, the results obtained for the two arrangement of fibers seems to be the same. Furthermore, the peak stress concentration during the transient time is higher (50%, for $r = 3$) in a lamina as compared to those of a laminate. Results show that for a single type fiber, the peak static and dynamic stress concentrations within a laminate, with an inside crack, occur at the top or bottom layer bounding the cracked layer. For a laminate with a surface crack (crack at the top or bottom layer) the

dynamic stress concentration is increased (for $r = 1$, the increase is about 18%). Moreover, an increase in the ratio of volume fraction V_m/V_f only advances the occurrence peak values of K_r . As a single type laminate is hybridized, the layers with LM fibers bounding the cracked layer, experience more stress concentrations. The opposite is true if the cracked layer is composed of HM fibers. Here, hybridization tends to even out the dynamic stress concentration within the laminate. For a crack initiating in an LM layer, the peak dynamic overshoot occurs at the crack tip. Due to the size of the resulting crack, the peak stress concentration can either take place in the layer adjacent to crack or at the crack tip.

Acknowledgment

The authors wish to thank the Ahvaz Branch, Islamic Azad University for the financial support. The authors would like to thank all the editors and reviewers for their comments in the development and improvement of this paper.

References

[1] M. Rezayat, M. Bahreman, M. Parsa, H. Mirzadeh, and J. Cabrera, "Modification of As-cast Al-Mg/B4C composite by addition of Zr", *Journal of Alloys and Compounds*, Vol. 685, pp. 70-77, (2016).

[2] M. Rezayat, M. Gharechomaghlu, H. Mirzadeh, and M. H. Parsa, "A comprehensive approach for quantitative characterization and modeling of composite microstructures", *Applied Mathematical Modelling*, Vol. 40, No. 19-20, pp. 8826-8831, (2016).

[3] E. Yousefi, A. Sheidaei, M. Mahdavi, M. Baniassadi, M. Baghani, and G. Faraji, "Effect of nanofiller geometry on the energy absorption capability of coiled carbon nanotube composite material", *Composites Science and Technology*, Vol. 153, pp. 222-231, (2017).

- [4] B. Sadeghi, M. Shamanian, F. Ashrafizadeh, P. Cavaliere, and A. Rizzo, "Friction stir processing of spark plasma sintered aluminum matrix composites with bimodal micro- and nano-sized reinforcing Al₂O₃ particles", *Journal of Manufacturing Processes*, Vol. 32, pp. 412-424, (2018).
- [5] J. M. Hedgepeth, "Concentration in a filamentary structure", *NASA TND-882*, (1961).
- [6] J. M. Hedgepeth, and P. Van Dyke, "Local Stress Concentrations in Imperfect Filamentary Composite Materials", *Journal of Composite Materials*, Vol. 1, No. 3, pp. 294-309, (1967).
- [7] C. M. Landis, M. A. McGlockton, and R. M. McMeeking, "An Improved Shear Lag Model for Broken Fibers in Composite Materials", *Journal of Composite Materials*, Vol. 33, No. 7, pp. 667-680, (1999).
- [8] J. N. Rossettos and M. Shishesaz, "Stress concentration in fiber composite sheets including matrix extension", *Journal of Applied Mechanics*, Vol. 54, pp. 334-342, (1987).
- [9] J. E. David Reedy, "Fiber Stresses in a Cracked Monolayer: Comparison of Shear-Lag and 3-D Finite Element Predictions", *Journal of Composite Materials*, Vol. 18, No. 6, pp. 595-607, (1984).
- [10] Z. Xia, T. Okabe, and W. A. Curtin, "Shear-lag versus finite element models for stress transfer in fiber-reinforced composites", *Composites Science and Technology*, Vol. 62, No. 9, pp. 1141-1149, (2002).
- [11] H. Fukuda, "An advanced theory of the strength of hybrid composites", *Journal of Materials Science*, Vol. 19, No. 3, pp. 974-982, (1984).
- [12] H. Fukuda, "Stress concentration factors in unidirectional composites with random fiber spacing", *Composites Science and Technology*, Vol. 22, No. 2, pp. 153-163, (1985).
- [13] H. Fukuda, and T. W. Chou, "Stress Concentrations in a Hybrid Composite Sheet", *Journal of Applied Mechanics*, Vol. 50, pp. 845-848, (1983).
- [14] D. Larom, C. T. Herakovich, and J. Aboudi, "Dynamic response of pulse loaded laminated composite cylinders", *International Journal of Impact Engineering*, Vol. 11, No. 2, pp. 233-248, (1991).
- [15] E. Mirshekari, *Transient Response and Stress Distributions in a Laminate Subjected to an internal Crack*, M.Sc. Thesis, Faculty of engineering, Shahid Chamran University, Iran, (2009).
- [16] A. Reza, H. M. Sedighi, and M. Soleimani, "Dynamic load concentration caused by a break in a Lamina with viscoelastic matrix", *Steel and Composite Structures*, Vol. 18, No. 6, pp. 1465-1478, (2015).
- [17] S. Souad, B. Serier, F. Bouafia, B. A. B. Boudjra, and S. S. Hayat, "Analysis of the stresses intensity factor in alumina-Pyrex composites", *Computational Materials Science*, Vol. 72, pp. 68-80, (2013).
- [18] J. Aboudi, "Transient response of piezoelectric composites caused by the sudden formation of localized defects", *International Journal of Solids and Structures*, Vol. 50, No. 16-17, pp. 2641-2658, (2013).
- [19] A. Reza and M. Shishesaz, "Transient load concentration factor due to a sudden break of fibers in the viscoelastic PMC under tensile loading", *International Journal of Solids and*

- [20] *Structures*, Vol. 88-89, pp. 1-10, (2016).
D. M. Causon and C. G. Mingham, *Introductory Finite Difference Methods for PDEs*: Ventus Publishing ApS, (2010).

How to cite this paper:

E. Mirshekari, A. Reza, “Dynamic stress concentration in a hybrid composite laminate subjected to a sudden internal break” *Journal of Computational and Applied Research in Mechanical Engineering*, Vol. 9, No. 1, pp. 153-167, (2019).

DOI: 10.22061/jcarme.2018.2604.1259

URL: http://jcarme.sru.ac.ir/?_action=showPDF&article=821

